

1 Impact of periconceptional and gestational vitamin D3 restriction on fetal folliculogenesis
2 and anti-mullerian hormone secretion using sheep as a model

3 E. C. Mbegbu^{1,7*}; M. Salavati^{2,7}; L. O. Aka³; I. R. Obidike¹; J. C. Y. Tang^{4,5}; W. D. Fraser^{4,5};
4 M.A. Hanson⁶; L. R. Green⁶; A. A. Fouladi-Nashta⁷

5 ¹ Veterinary Physiology and Biochemistry, University of Nigeria, Nsukka, Nigeria;

6 ² Dairy Research Innovation Centre, South and West Faculty, Scotland's Rural College, Dumfries,
7 United Kingdom;

8 ³ Veterinary Biosciences, St Matthew's University, Grand Cayman, Cayman Islands

9 ⁴ Bioanalytical Facility, Norwich Medical School, University of East Anglia, Norwich Research Park,
10 Norwich, UK

11 ⁵ Departments of Clinical Biochemistry, Diabetes and Endocrinology, Norfolk and Norwich University
12 Hospital NHS Foundation Trust, Colney Lane, Norwich, UK

13 ⁶ Institute of Developmental Sciences, Faculty of Medicine, University of Southampton,
14 Southampton, United Kingdom;

15 ⁷ Comparative Biomedical Sciences, Royal Veterinary College, London, United Kingdom;

*16 *Corresponding author*

Abstract

Ovarian reserve is a reflection of the overall female reproductive potential. Vitamin D status has been suspected to influence fetal development and female fertility. As maternal diet during pregnancy can affect fetal development and future fertility, we hypothesized that periconceptional and gestational vitamin D restriction could affect folliculogenesis and AMH secretion in the offspring. Nineteen sexually mature Welsh mountain ewes were randomly assigned to vitamin D3 deficient (VDD, n=10) and vitamin D3 control (VDC, n=9) diets from 17 days (d) before mating, up to 127-130 d of gestation, when fetal ovaries were collected (3 from VDC and 6 from VDD). Serum 25(OH)D3 concentrations were lower in VDD compared with VDC ($P < 0.05$). Relative to total follicle number, the percentage of primordial follicles was higher ($P < 0.05$), while the percentage of primary follicles was lower ($P < 0.05$) in VDD group compared with VDC group fetal ovaries. The integrated density value and percentage of affected area in TUNEL staining in VDD group did not vary from VDC group fetal ovaries ($P > 0.05$). Relative expression of *AMH* mRNA and AMH protein in VDD fetal ovaries were not statistically different compared with controls ($P > 0.05$). The relative expression of *VDR* mRNA were lower in VDD compared with VDC group fetal ovaries ($P < 0.05$). These data indicate that maternal vitamin D dietary restriction is associated with ovarian tissue stemness and increased primordial follicle number, but does not promote normal follicle recruitment or development in sheep fetal ovaries.

Key words: Anti-Mullerian Hormone, Apoptosis, Fetal Ovaries, Folliculogenesis, Sheep, Vitamin D

Running Title: *Impact of vitamin D status on sheep fetal ovarian folliculogenesis*

1. Introduction

The pool of primordial follicles is established during fetal life and represents the reproductive capacity of most female mammals, otherwise known as the ovarian reserve (Priya *et al.*, 2021). The ovarian reserve is usually estimated through determination of serum concentrations of Anti-Müllerian Hormone (AMH) (Jamil *et al.*, 2016), a member of the transforming growth factor-beta superfamily glycoprotein, produced by granulosa cells of primary, pre-antral (secondary), and small antral follicles in the ovaries (Kristensen, *et al.*, 2014). Ordinarily, AMH inhibits the loss of the oocyte pool by inhibiting the recruitment of primordial follicles and slowing down follicle growth (Rudnicka *et al.*, 2021). Thus, *Amh*-null gene mutations result in early depletion of the stock of the oocyte pool in the mouse ovary, with consequent short duration of the reproductive life span (Bedenk *et al.*, 2020).

The active form of Vitamin D, 1,25-dihydroxyvitamin D₃, mediates its action through the vitamin D receptor (VDR); a member of the steroid/thyroid nuclear hormone receptor superfamily (Johnson and DeLuca, 2001). Nuclear localization of VDR has been reported in most female reproductive organs, including the endometrium, myometrium, ovary, mammary glands, cervix, and placenta, indicating active signaling in these tissues (Vienonen *et al.*, 2004). The active form of Vitamin D, 1,25-dihydroxyvitamin D₃, acts via the VDR during and after fetal life to elicit its physiological effects (Pludowski *et al.*, 2013). Vitamin D deficiency has been linked to poor ovarian reserve and poor developmental ability in ovarian follicles (Arefi *et al.*, 2018).

A functional vitamin D response element was identified in the promoter region of the human *AMH* gene, and direct association of VDR with the *AMH* promoter has been demonstrated in prostate cancer cell lines (Malloy, *et al.*, 2009). A high correlation has been reported between serum concentrations of AMH and 25(OH)D in women given daily supplements of Vitamin D (Dennis

1 *et al.*, 2012). In cumulus oocytes complexes retrieved during IVF procedures, 1,25-
2 dihydroxyvitamin D₃ decreased AMH sensitivity in granulosa cells, as well as AMHR-II and FSH
3 receptor mRNA expression, but increased 3-βHSD mRNA expression (Merhi *et al.*, 2014).
4 However, it is not known whether a regulatory relationship exists between 1,25-dihydroxyvitamin
5 D₃, VDR and AMH in the granulosa cells of the ovary, hence the reason for this research.

6 This study was designed to test the hypothesis that maternal vitamin D restriction affects
7 primordial follicle recruitment, folliculogenesis and AMH expression in the ovaries of sheep
8 fetuses prenatally exposed to dietary vitamin D deficiency.

9 **2. Materials and methods**

10 ***2.1 Experimental design***

11 Nineteen normally cycling mature first parity Welsh Mountain ewes (body condition score of 2.5-
12 3.0) were housed individually in barns at The Royal Veterinary College (Hertfordshire UK), with
13 no direct sunlight. After a minimum of 8 weeks acclimatization to facilities, the ewes were
14 synchronized to a common stage of estrus by insertion of medoxyprogesterone acetate for 10 days
15 followed by removal of the sponges. Successfully mated ewes were randomly assigned to one of
16 two nutritional treatment groups, vitamin D control (VDC) and experimental vitamin D deficient
17 (VDD) groups. VDC group (n=9 ewes) were fed complete pelleted diet containing 2,000 IU/kg
18 body weight of vitamin D (P316, Charwood Milling). VDD group (n=10 ewes) were fed with a
19 customized brand of P316 prepared with 0 IU/kg body weight of vitamin D₃ supplement. Feed
20 and water were available *ad libitum* from 17 days prior to natural mating, and continued throughout
21 the entire gestation period. The study protocol was approved by UK government Home Office and
22 RVC local ethics committee (PPL 30/3003 LR Green).

2.2 Tissue Collection and Processing

At 128 days of gestation (dGA), all singleton-bearing ewes were euthanized by an overdose of 40-60 mL I.V. 200mg/mL pentobarbitone sodium. There were 3 VDC and 6 VDD group female fetuses. Blood samples were collected for fetal serum 25(OH)D concentration measurement. Fetal ovaries were collected and weighed. The right ovary of each fetus was snap-frozen in liquid nitrogen and stored at -80°C pending mRNA extraction, and the left ovary was fixed in formalin (10%) and embedded in paraffin blocks by standard methods. Five micrometer serial sections were applied to hydrochloric acid (HCL)-treated, Poly-L-Lysine-coated glass slides (Scientific Laboratory Supplies, UK) and left to dry overnight at 37°C in the oven.

2.3 Measurement of Serum Vitamin D

25(OH)D measurements were performed at the Bioanalytical Facility, University of East Anglia (Norwich, UK) under Good Clinical and Laboratory Practice conditions. The concentrations of 25(OH)D₂ and 25(OH)D₃ were determined in fetal serum samples by liquid chromatography tandem mass spectrometry (HPLC–MS/MS) as previously described (Cleal *et al.*, 2017). Total 25(OH)D is calculated from the sum of 25(OH)D₂ and 25(OH)D₃. The assays were calibrated using standards aligned to the SRM972a from the National Institute of Science and Technology (NIST). The inter/intra-assay coefficient of variation (%CV) across the assay range of 2.5-300 nmol/L was between 3.9-10.8%. The assay showed <12% accuracy bias against the target method on the vitamin D external quality assessment (DEQAS) scheme.

2.4 Histological analysis

Tissue sections were de-waxed in HistoClear II (National Diagnostics, Hull, UK), rehydrated in descending grades of ethanol, and counterstained in H&E. Sections were subsequently dehydrated in ascending grades of alcohol and HistoClear II) for 2 minutes each, before permanent mounting

with DPX mountant (BDH Laboratory, England, UK). Every 10th section was used for light microscopy and histomorphometric analysis. Images were collected using a DM4000Bright field upright microscope and DC500 colour camera with Leica Application Suite software version 2.8.1 for Windows (Leica Microsystems, USA), merged using Adobe Photoshop CC (Adobe Systems). The objective lens used was 5x HC PL FLUOTAR PH1 (NA=0.3). The number of ovarian follicles in serially sectioned H&E-stained fetal ovaries were calculated using ratio estimation method with the aid of ImageJ software as previously described (McClellan *et al.*, 2003). An estimate of the total number of follicles at each maturational stage within the entire ovary was calculated using the formula:

$$Nt = Nf \times St \times ts / (So \times do);$$

where Nt = total calculated number of follicles of one type within the ovary; Nf = total number of follicles counted from every section observed; St = total number of sections in the ovary; ts = thickness of the section (µm); So = total number of sections observed; and do = mean oocyte diameter of that follicular type (across all sections).

2.5 TUNEL Assay

Formalin-fixed ovary sections were de-waxed in histoclear II, and rehydrated in descending grades of alcohol and PBS containing 1% BSA for 10 minutes. Tissues were permeabilized with 1% Triton X-100 in PBS for 5 minutes. After washing, apoptotic cells were detected using the In Situ Cell Death Detection Kit (Fluorescein) (Roche Life Sciences, UK) according to the manufacturer's instruction. The sections were then washed in PBS, counterstained with 10µg/ml Hoechst 33422 (ThermoFisher Scientific, Paisley, UK) for 5 minutes at room temperature in an opaque humidified chamber, and mounted with Vectashield mounting medium (without DAPI) (Vector Laboratories, Peterborough, UK) and observed using a Leica fluorescent microscope. Images were saved in raw

format with maximum quality setting (TIFF, 0-255 pixel density) Intensity of the fluorescent staining was quantified using the colour deconvolution tool of ImageJ software (Schindelin et al, 2012).

2.6 RNA Extraction and cDNA Synthesis

Total RNA was extracted from the frozen ovaries using the RNeasy Mini Kits (QIAGEN, Hilden, Germany). Briefly, tissue lysates were made by disrupting and homogenizing 30 mg each of crushed ovarian tissues samples with 600 μ L of RNA-binding guanidine isothiocyanate-containing (GITC) RLT buffer and centrifuged at 13,000xg for 3 minutes. The supernatant was then mixed well with 600 μ L of 70% ethanol, and transferred to the RNA-easy spin columns. Washes and centrifugation were carried out according to the manufacturer's instruction, and RNAs were finally eluted in 30 μ L of nuclease free water and the concentration was measured by a TECAN plate reader (TECAN, Switzerland). RNA concentration (ng/ μ L) was normalized to 18s rRNA among samples by dilution to 50 ng in 8 μ L volume

Genomic DNA carryover and possible contaminants were eliminated from the validated RNA samples by DNase treatment using the standard procedure described for the RNase-free DNase kit (Promega, Madison, WI, USA). With strict adherence to the manufacturer's instructions in the GoScript reverse transcription system Technical manual (Promega, Madison, WI, USA), reverse transcription of total RNA samples was immediately followed by the reverse transcription of the total RNA to complementary DNA (cDNA) to avoid the risk of RNA degradation. The same amount of RNA (1 μ g) from all the samples were reverse transcribed at the same time under similar conditions to minimize variability between experimental replicates. A master mix of RT reagents was prepared once to minimize potential variation. The resultant cDNA products were cooled on ice and stored at -20°C for subsequent PCR experiments.

2.7 Measurement of gene expression by Conventional PCR and RT-qPCR

Relative quantification of mRNA expression of the target genes was performed on a Bio-Rad CFX96 Real-time qPCR Thermal Cycler (Bio-Rad, Hercules, CA, USA). For all the RT-qPCR experiments, 20 µL of qPCR mixtures placed in 0.1 mL white PCR tubes were prepared thus: 10µL 2x qPCRBIO SyGreen Mix (PCR Biosystems Ltd, London, UK), 1.6 µL of 0.4 µM combined forward and reverse primers (final primer concentration was 0.032 µM; Table 1), 25 ng of cDNA, and 7.9µL of nuclease free water (NFW). The no template control (NTC) contained 0.5µL of NFW instead of cDNA. All RT-qPCR assays were performed in duplicates. General cycling conditions were as follows: initial denaturing at 95°C for 10 minutes; 40 cycles of 15 seconds at 95°C; 30 seconds at 57-62°C 30 seconds at 60°C, depending on the target gene; fluorescent reading at the end of each cycle at 80°C; final extension for 5 seconds at 60°C; melt cycle from 60-95°C, held for 1 second every increase in °C and read every 5 seconds. The 18s Ribosomal RNA (18s rRNA) gene was selected as the most stable housekeeping gene using geometric mean ANOVA test (non-significance) methodology between different cDNA samples in comparison to β Actin and GAPDH (unpublished data). The values of amplification curves were normalized to the values of amplification curves of *18S rRNA*, and compared between groups using the $2^{-\Delta\Delta Ct}$ method (Livak and Schmittgen, 2001).

RT-qPCR finding was verified by amplification of the selected cDNAs using Qiagen Multiplex conventional PCR kit and G-Storm thermal cycler (Gene Technologies, Essex, UK). 25µL PCR reactions were identically prepared by mixing 12.5µL Qiagen Multiplex PCR Master Mix, 2.5 µL of 2 µM combined forward and reverse primers (final primer concentration was 0.2 µM; Table 1), 50 ng of cDNA, and 9µL of NFW. The PCR products were visualized by agarose gel electrophoresis and captured in a Syngene G Box with the imaging software (Syngene, Cambridge,

UK). *AMH* signal was measured by densitometry and standardized against the *18srRNA* signal using a digital imaging and analysis system (AlphaEase, Alpha Innotech Corporation; San Leandro, CA, USA).

2.8 Immunohistochemistry (IHC) for AMH

Fixed tissue sections were deparaffinized, rehydrated and antigen retrieval and endogenous peroxidase activity blocked. Slides were blocked in 10% normal goat serum (Vectastain Elite ABC kit, Vector Laboratories) with 4% bovine serum albumin (BSA) in PBS for 1 hour in a humidified chamber. Sections were incubated with monoclonal mouse anti-human AMH antibody (Antibodies online, Atlanta, GA, USA Cat. No. ABIN317404) diluted 1:50 in PBS+BSA overnight at 4°C in a humidified chamber. The negative control was treated with PBS+BSA omitting the primary antibody. Sections were washed in PBS and incubated with 1:200 goat anti-mouse IgG diluted in PBS for 60 minutes; washed in PBS and treated with Avidin-Biotin complex solution for 30 minutes at room temperature. The sections were then washed and developed with 3% (v/v) 3,3-diaminobenzidine (DAB) chromogen in peroxidase substrate diluent for 3 minutes in a dark chamber. The DAB staining was stopped by washing the section with distilled water. Slides were counterstained with Haematoxylin, dehydrated and permanently mounted for microscopy as earlier stated. Intensity of the AMH staining was quantified using the colour deconvolution tool, while the percentage of affected area was determined using ImageJ area measurement tool.

2.9 Statistical Analysis

SPSS version 21.0 for Windows (IBM Corp, Armonk, NY, USA 2012) was used for the statistical analyses. Data obtained were analyzed using independent sample t-test and two-way ANOVA. Significance was accepted when $P < 0.05$, and trends defined as $0.05 < P < 1.0$. The data in tables and graphs are presented as mean \pm standard errors of the mean (S.E.M).

3. Results

3.1 Fetal serum 25(OH)D concentration

By 127 dGA, the supplementation resulted in maternal serum 25(OH)D concentrations of 128.5±14.4 nmol/L (VDC) and 102.9±8.1 nmol/L (VDD) (Table 2). Fetal serum concentration of 25(OH)D₃ was lower in VDD compared with the VDC group (15.0±1.9 nmol/L (VDD) vs 29.3±6.1 nmol/L (VDC), $P = 0.02$). However, the serum concentration of 25(OH)D₂ {24.4±2.9 nmol/L (VDD) vs 33.5±10.2 nmol/L (VDC), $P = 0.28$ }; and the total 25(OH)D {39.4±4.5 nmol/L (VDD) vs 62.8±14.6 nmol/L (VDC), $P = 0.08$ } did not differ between the groups respectively; **Figure 1**).

3.2 Fetal and ovarian weights

Absolute body weights of fetuses were not significantly different for VDD and VDC fetuses ($P > 0.05$) (**Table 3**). The ovarian (left, right and average) weight to fetal weight ratios were not significantly different between VDD and VDC groups ($P > 0.05$; **Table 3**).

3.3 Fetal ovarian histomorphometry

The total number of sections obtained from entire serial sectioning of the fetal ovaries were 89±4 (VDC) and 99±7 (VDD) respectively. Folliculogenesis was detected up to the early antral stage in fetal ovaries from both VDC and VDD groups (**Figure 5A & 5B**). Estimates of the total number of follicles (**Figure 2A**), primordial follicles (**Figure 2B**), primary follicles (**Figure 2C**), secondary follicles (**Figure 2D**) and antral follicles (**Figure 2E**) in ovaries were not significantly ($P > 0.05$) different between diet groups. However, there was a significantly higher percentage of primordial follicles when compared with the total follicle ($P = 0.05$; **Figure 2F**), and a lower percentage of primary follicles in relation to the total follicle ($P = 0.04$; **Figure 2G**) in VDD group compared with VDC fetal ovaries.

3.4 TUNEL Assay for Apoptosis in fetal ovaries

There was no significant difference in the TUNEL staining density (integrated density value, IDV) ($P > 0.05$; **Figure 3A**) and percentage of affected area ($P > 0.05$; **Figure 3B**) between the VDD and VDC groups.

3.5 AMH and VDR mRNA levels in fetal ovaries

There was no significant difference in the relative *AMH* mRNA expression in VDD compared with VDC fetal ovaries ($P < 0.05$; **Figure 4A, 4C, 4D**). Relative *VDR* mRNA expression was lower in fetal ovaries of VDD group compared with the VDC group ($P = 0.006$; **Figure 4B**).

3.7 AMH protein density in fetal ovaries

AMH protein was detected in the granulosa cells layers of the growing follicles in VDC (**Figure 5A**) and VDD (**Figure. 5B**) fetal ovaries. However, there was no significant difference between the VDD and VDC group in the area stained positive for AMH, either as percentage of entire follicular area ($P > 0.05$; **Figure 5D**) or per mm² of stained follicles ($P > 0.05$; **Figure 5E**).

4. Discussion

Developing fetuses depend on their mother for supply of vitamin D, through placental transfer (Cleal *et al.*, 2017). This research work showed that periconceptional and gestational restriction of dietary 25(OH)D decreased the fetal serum 25(OH)D₃ and relative *VDR* mRNA expression, and folliculogenesis in female sheep fetuses. We observed that while *AMH* mRNA expression and TUNEL staining intensity did not vary, there was an increase in the percentage of primordial follicles, and a decrease in the percentage of primary follicles in ovaries of fetuses harvested from dams exposed to a vitamin D deficient diet.

Serum 25(OH)D concentrations have been correlated with a variety of reproductive parameters in

1 females (Voulgaris *et al.*, 2017). The total follicular numbers observed in this study are consistent
2 with previous reports of sheep at a similar stage of gestation approximately 100,000 at 130 dGA
3 and 82,000 at the time of birth in Booroola ewes (Van den Hurk and Zhao, 2005). The percentage
4 of primordial follicles in relation to total follicles at 127-130 dGA was significantly higher in VDD
5 compared with the VDC group fetal ovaries. However, the percentage of primary follicles number
6 in relation to total follicles was significantly reduced in VDD compared with the VDC group fetal
7 ovaries. The primordial follicle pool is determined early in life, and primordial follicles are
8 recruited to join the growing follicle class at day 3-4 post-natal life in the rodents (Rajah *et al.*,
9 1992), 154th day of gestation in humans (Fulton *et al.*, 2005), and 75th day of gestation in sheep
10 (Juengel *et al.*, 2002). These data suggest that there was interference in pathways or mechanisms
11 for optimal recruitment and progression of primordial follicles to primary stage in the VDD group.
12 The increased number of primordial follicles in the VDD group fetuses could arise from increased
13 germ cell formation and migration to the genital ridge, without commensurate recruitment into the
14 growing follicles pool or due to reduced follicular demise in VDD fetuses (Abdelbaset-Ismail *et*
15 *al.*, 2016).

16 Studies in humans and rodents have shown that 1,25-dihydroxyvitamin D3 during bone
17 remodeling and tumorigenic processes inhibits NOTCH and Wnt signaling required for stemness
18 and development, or downregulates of octamer-binding transcription factor 4 (OCT-4) and
19 NANOG (Clevers and Nusse, 2012; Larriba *et al.*, 2014). NOTCH/Wnt pathways regulate early
20 ovary development and follicle formation, and their inhibition would be expected to increase
21 primordial follicle numbers (Jääskeläinen *et al.*, 2010; Vanorny *et al.*, 2014), while an increase in
22 OCT4/NANOG levels may lead to fewer primordial germ cells (PGCs), or premature PGC
23 differentiation, leading to reduced numbers of oocytes to form follicles. Consistent with this idea,

1 Xu *et al.* (2016) reported that *in vitro* vitamin D3 supplementation promotes survival and growth
2 of follicles harvested from ovarian tissues from adult female rhesus macaques (*Macaca mulatta*).

3 The elevated percentage of primordial follicles in VDD group fetal ovaries compared to VDC in
4 the current study could be due to alteration in apoptotic pathways. Apoptosis is responsible for up
5 to 99% loss of the ovarian follicle pool, and occurs in the germ cells and supporting somatic cells
6 in a developmental stage-specific manner (Santos *et al.*, 2013). During early fetal life, apoptosis
7 occurs predominantly in the germ cells and surrounding somatic cells, whereas later in
8 development, once follicle formation is largely complete, apoptosis is more commonly detected in
9 the granulosa cells (Santos *et al.*, 2013). The ovaries used in this experiment were harvested from
10 fetuses; hence the increase in the primordial follicles in VDD group could be due to decreased
11 programmed germ and somatic cell death.

12 Our observation that both the expression of *AMH* gene and the population of the AMH-secreting
13 follicles did not differ between the diet groups appears consistent with previous work which
14 demonstrated that the number and size of the AMH-secreting class of follicles is directly
15 proportional to the quantity of AMH produced (Gnoth *et al.*, 2015). However, previous studies in
16 prostate cancer cell lines have shown that Vitamin D may also up-regulate human *AMH* gene
17 (Malloy *et al.*, 2009). Our finding of a significant reduction in *Vitamin D receptor (VDR)* mRNA
18 expression in the VDD group fetal ovaries could be due to the decreased serum concentration of
19 biologically active form of vitamin D which determines the degree of *VDR* expression (La Marra
20 *et al.*, 2017). An increase in *VDR* mRNA and protein expressions following 1,25-dihydroxyvitamin
21 D3 treatment in hen was also recorded by Wojtusik and Johnson, 2012. It remains possible that
22 other hormonal or transcriptional regulators co-impacted the gene expression level of the VDR
23 due to compensatory loop backs from D3 deficiency, which warrants further research.

In conclusion, our finding in sheep that lower fetal serum 25(OH)D3 concentration was associated with higher percentage of primordial follicles in relation to the total follicles and lower *VDR* expression could be consistent with a role for vitamin D, or specific circulating forms of it, in normal growth and development of the ovarian follicles. While the longer-term consequences were not tested, prenatal exposure of sheep fetuses to reduced vitamin D may have implications for fertility outcomes in postnatal life of female offspring in sheep.

Limitation of the study

Until puberty in mammals, folliculogenesis in fetal ovaries does not yield all the classes of follicles from primary to large antral follicles. Therefore, the expression of the anti-mullerian hormone in this study could have been influenced by the fact the ovaries were obtained from fetuses. Again, since the dams were naturally mated and not inseminated with sorted sperm cells, the number of female fetuses obtained was left to probability, hence we had only three female fetuses from the VDC group.

Acknowledgements

The authors thank Dr Daniel Hampshire, Dr Zhangrui Cheng and Dr Francesca Soutter for technical support.

Data availability

All the raw images from the study (H&E, TUNEL staining or IHC) are available upon request from the authors.

Authors' Roles

ECM, LRG, MAH and AFN conceived the study and designed experiments. JCYT, WDF, ECM, MS, and AFN performed the laboratory research and performed data analysis. ECM, MS, IRO,

LOA, and AFN interpreted the data. ECM, drafted the initial manuscript. All authors approved the final version of the paper

Funding

M.E.C. received from Tertiary Education Trust Fund (TETFund) AST&D University of Nigeria, Nsukka, with reference number UN/VC/T/19/N.2.

Conflict of interest

The authors declare that there is no conflict of interest that may be perceived as prejudicing the impartiality of the research reported.

References

- Abdelbaset-Ismail, A., Pedziwiatr, D., Suszyńska, E., Sluczanowska-Glabowska, S., Schneider, G., Kakar, S.S., & Ratajczak, M.Z. (2016). Vitamin D3 stimulates embryonic stem cells but inhibits migration and growth of ovarian cancer and teratocarcinoma cell lines. *Journal of Ovarian Research*, 9, 26.
- Arefi, S., Khalili, G., Iranmanesh, H., Farifteh, F., Hosseini, A., Fatemi, H.M., & Lawrenz, B. (2018). Is the ovarian reserve influenced by vitamin D deficiency and the dress code in an infertile Iranian population? *Journal of Ovarian Research*, 11(1), 62.
- Bedenk, J., Vrtačnik-Bokal, E., & Virant-Klun, I. (2020). The role of anti-Müllerian hormone (AMH) in ovarian disease and infertility. *Journal of Assisted Reproduction and Genetics*, 37(1), 89-100.
- Cleal, J., Hargreaves, M., Poore, K., Tang, J., Fraser, W., Hanson, M., & Green, L. (2017). Reduced fetal vitamin D status by maternal undernutrition during discrete gestational windows in sheep. *Journal of Developmental Origins of Health and Disease*, 8(3), 370-381.

1 Clevers, H., and Nusse, R. (2012). Wnt/ β -catenin signaling and disease. *Cell*, 149, 1192–1205.

2 Dennis, N.A., Houghton, L.A., Jones, G.T., van-Rij, A.M., Morgan, K., & McLennan, I.S. (2012).
3 The level of serum anti-Mullerian hormone correlates with vitamin D status in men and
4 women but not in boys. *Journal of Clinical Endocrinology and Metabolism*, 97(7), 2450-
5 2455.

6 Fulton, N., Martins da Silva, S.J., Bayne, R.A.L., & Anderson, R.A. (2005). Germ cell
7 proliferation and apoptosis in the developing human ovary. *Journal of Clinical*
8 *Endocrinology and Metabolism*, 90, 4664-4670.

9 Gnoth, C., Roos, J., Broomhead, D., Schiffner, J., Godehardt, E., Freundl, G., & Johnson, S.
10 (2015). Antimüllerian hormone levels and numbers and sizes of antral follicles in regularly
11 menstruating women of reproductive age referenced to true ovulation day. *Fertility and*
12 *Sterility*, 104(6), 1535–15343.

13 IBM Corp. Released 2012. IBM SPSS Statistics for windows, Version 21.0 Armonk, N.Y. IBM
14 Corp.

15 Jääskeläinen, M., Prunskaitė-Hyyryläinen, R., Naillat, F., Parviainen, H., Anttonen,
16 M., Heikinheimo, M., Liakka, A., Ola, R., Vainio, S., Vaskivuo, T.E., & Tapanainen, J.S.
17 (2010). WNT4 is expressed in human fetal and adult ovaries and its signaling contributes
18 to ovarian cell survival. *Molecular and Cellular Endocrinology*, 317(1-2), 106-111.

19 Jamil, Z., Fatima, S.S., Cheema, Z., Baig, S., & Choudhary, R.A. (2016). Assessment of ovarian
20 reserve: Anti-Mullerian hormone versus follicle stimulating hormone. *Journal of research*
21 *in medical sciences: The official journal of Isfahan University of Medical Sciences*, 21,
22 100.

- 1 Johnson, L.E., and DeLuca, H.F. (2001). Vitamin D receptor null mutant mice fed high levels of
2 calcium are fertile. *Journal of Nutrition*, 131(6), 1787-1791.
- 3 Juengel, J.L., Sawyer, H.R., Smith, P.R., Quirke, L.D., Heath, D.A., Lun, S., Wakefield, S.J., &
4 McNatty, K.P. (2002). Origins of follicular cells and ontogeny of steroidogenesis in ovine
5 fetal ovaries. *Molecular and Cellular Endocrinology*, 191(1), 1-10.
- 6 Kristensen, S.G., Andersen, K., Clement, C.A., Franks, S., Hardy, K., & Andersen, C.Y. (2014).
7 Expression of TGF-beta superfamily growth factors, their receptors, the associated SMADs
8 and antagonists in five isolated size-matched populations of pre-antral follicles from
9 normal human ovaries. *Molecular Human Reproduction*, 20(4), 293-308.
- 10 La Marra, F., Stinco, G., Buligan, C., Chiriaco, G., Serraino, D., Di Loreto, C., & Cauci, S. (2017).
11 Immunohistochemical evaluation of vitamin D receptor (VDR) expression in cutaneous
12 melanoma tissues and four VDR gene polymorphisms. *Cancer biology & medicine*, 4(2),
13 162-175.
- 14 Larriba, M.J., González-Sancho, J.M., Bonilla, F., & Muñoz, A. (2014). Interaction of vitamin D
15 with membrane-based signaling pathways. *Frontiers in Physiology*, 5, 60.
- 16 Livak, K.J., & Schmittgen, T.D. (2001). Analysis of relative gene expression data using real-time
17 quantitative PCR and the $2^{-\Delta\Delta Ct}$ method. *Methods*, 25, 402-408.
- 18 Malloy, P.J., Peng, L., Wang, J., & Feldman, D. (2009). Interaction of the Vitamin D Receptor
19 with a Vitamin D Response Element in the Müllerian-Inhibiting Substance (MIS)
20 Promoter: Regulation of MIS Expression by Calcitriol in Prostate Cancer
21 Cells. *Endocrinology*, 150(4), 1580-1587.

- 1 McClellan, K.A., Gosden, R., & Taketo, T. (2003). Continuous loss of oocytes throughout meiotic
2 prophase in the normal mouse ovary. *Developmental Biology*, 258(2), 334-348.
- 3 Merhi, Z., Doswell, A., Krebs, K., & Cipolla, M. (2014). Vitamin D alters genes involved in
4 follicular development and steroidogenesis in human cumulus granulosa cells. *The Journal*
5 *of Clinical Endocrinology and Metabolism*, 99(6), 1137-1145.
- 6 Pludowski, P., Holick, M.F., Pilz, S., Wagner, C. L., Hollis, B. W., Grant, W. B., Shoenfeld, Y.,
7 Lerchbaum, E., Llewellyn, D. J., Kienreich, K., & Soni, M. (2013). Vitamin D effects on
8 musculoskeletal health, immunity, autoimmunity, cardiovascular disease, cancer, fertility,
9 pregnancy, dementia and mortality-a review of recent evidence. *Autoimmunity reviews*,
10 2(10), 976-89.
- 11 Priya, K., Setty, M., Babu, U.V., & Pai, K.S.R. (2021). Implications of environmental toxicants
12 on ovarian follicles: how it can adversely affect female fertility? *Environ Sci Pollut Res*
13 *Int.*, 28(48), 67925-67939.
- 14 Rajah, R., Glaser, E.M., & Hirshfield, A.N. (1992). The changing architecture of the neonatal rat
15 ovary during histogenesis. *Developmental Dynamics*, 194, 177-192.
- 16 Rudnicka, E., Kunicki, M., Calik-Ksepka, A., Suchta, K., Duszewska, A., Smolarczyk, K., &
17 Smolarczyk, R. (2021). Anti-Müllerian Hormone in Pathogenesis, Diagnostic and
18 Treatment of PCOS. *Int J Mol Sci.*, 22(22), 12507.
- 19 Santos, S.S., Ferreira, M.A., Pinto, J.A., Sampaio, R.V., Carvalho, A.C., Silva, T.V., Costa, N.N.,
20 Cordeiro, M.S., Miranda, M.S., Ribeiro, H.F., & Ohashi, O. M. (2013). Characterization
21 of folliculogenesis and the occurrence of apoptosis in the development of the bovine fetal
22 ovary. *Theriogenology*, 79(2), 344-350.

- Schindelin, J., Arganda-Carreras, I., Frise, E., Kaynig, V., Longair, M., Pietzsch, T., Preibisch, S., Rueden, C., Saalfeld, S., Schmid, B., Tinevez, J. Y., White, D. J., Hartenstein, V., Eliceiri, K., Tomancak, P., & Cardona, A. (2012). Fiji: an open-source platform for biological-image analysis. *Nature methods*, 9(7), 676–682.
- Van den Hurk, R., and Zhao, J. (2005). Formation of ovarian follicles and their growth, differentiation and maturation within ovarian follicles. *Theriogenology*, 63, 1717–1751.
- Vanorny, D.A., Prasasya, R.D., Chalpe, A.J., Kilen, S.M., & Mayo, K.E. (2014). Notch signaling regulates ovarian follicle formation and coordinates follicular growth. *Molecular Endocrinology*, 28(4), 499-511.
- Vienonen, A., Miettinen, S., Blauer, M., Martikainen, P.M., Tomas, E., Heinonen, P.K., & Ylikomi, T. (2004). Expression of nuclear receptors and cofactors in human endometrium and myometrium. *Journal of the Society for Gynecologic Investigation*, 11, 104-112.
- Voulgaris, N., Papanastasiou, L., Piaditis, G., Angelousi, A., Kaltsas, G., Mastorakos, G., & Kassi, E. (2017). Vitamin D and aspects of female fertility. *Hormones*, 16, 5-21.
- Wojtusik, J., & Johnson, P.A. (2012). Vitamin D regulates anti-Mullerian hormone expression in granulosa cells of the hen. *Biology of Reproduction*, 86(3), 91.
- Xu, J., Hennebold, J.D., & Seifer, D.B. (2016). Direct vitamin D3 actions on rhesus macaque follicles in three-dimensional culture: assessment of follicle survival, growth, steroid and anti-Müllerian hormone production. *Fertility and Sterility*, 106(7), 1815–1820.

1 **Figure legends**

2 **Figure 1:** Fetal serum levels of 25OH-D₂ and D₃ following maternal restriction of dietary vitamin
3 D₃. There was a significant reduction in 25OHD₃ in the VDD fetuses. Results are presented as the
4 means \pm S.E.M. Asterisks indicate significant (* $P < 0.05$) difference from VDC group (n=3 for
5 VDC, n=6 for VDD).

6 **Figure 2:** Ovarian follicles count in fetuses following VDC and VDD periconceptional and
7 gestational maternal diet. Total follicles count (A), Primordial follicles count (B), Primary follicles
8 count (C), Secondary follicles count (D), and Antral follicles count (E). Primordial (F), Primary
9 (G), Secondary (H) and Antral (I) were also expressed as percentage of the Total follicles. Maternal
10 vitamin D deficiency increased the primordial follicles, but decreased the primary follicles when
11 expressed as a percentage of the total follicles counted. Results are presented as the means \pm S.E.M.
12 Asterisks indicate significant (* $P < 0.05$) differences from VDC group (n=3 for VDC, n=6 for
13 VDD).

14 **Figure 3:** TUNEL staining for apoptotic cells in fetal ovary following periconceptional and
15 gestational exposure to VDC and VDD diets. Bright green-coloured dots represent apoptotic cells
16 (white arrow). There was no significant difference ($P > 0.05$) in the TUNEL staining density (A)
17 and percentage of affected area (B) between the treatment groups. Results are presented as the
18 means \pm S.E.M. Scale bar: 50 μ m (n=3 for VDC, n=6 for VDD).

19 **Figure 4:** Expression of *AMH* and *VDR* in fetal ovaries following VDC and VDD periconceptional
20 and gestational maternal diet. Relative mRNA expression of *AMH* (A) and *VDR* (B) as determined
21 by RT-qPCR. Conventional multiplex RT-PCR for *AMH* (C), (expected product size 216bp,
22 observed; \simeq 216bp) and *18S* (expected product size 216bp, observed; \simeq 216bp); AlphaEaseFC

Densitometry of the *AMH* RT-PCR products (D) showing comparable ($P > 0.05$) Integrated Density Values (IDV) as ratio to the corresponding internal control within the sample (18S); Results are presented as the means \pm S.E.M (n=3 for VDC, n=6 for VDD).

Figure 5: Immunohistochemical staining of AMH in fetal ovaries following VDC (A) and VDD (B) periconceptional and gestational maternal diet. IgG control (C). Pd=Primordial follicle, P=Primary follicle, S=Secondary follicle, A=Antral follicle. There was no significant difference ($P > 0.05$) in the % follicular area stained (D) and AMH DAB signal per surface area of DAB-stained follicles (E) between the treatment groups. Results are presented as the means \pm S.E.M, Scale bar: 50 μ m (n=3 for VDC, n=6 for VDD).

TABLES AND FIGURES

Table 1: Sequences of the primers used in PCR Experiments

Gene name	Sequence 5'-3' (Forward and Reverse)	Product size	Accessionnumber
<i>18s</i>	F: GCTCGCTCCTCTCCTACTTG R: CGTTTCTCAGGCTCCCTCT	326bp	AY_7531901
<i>AMH</i>	F: GTGGTGCTGCTGCTAAAGATG R: TCGGACAGGCTGATGAGGAG	216bp	XM_0040093771
<i>VDR</i>	F: ACCACAAGACCTACGATGACAC R: TCACTCTGATGCTGGTTGAAA	205bp	NC_0194602

Table 2: Maternal Serum 25(OH)D (nmol/L)

GROUP	25(OH)D2	25(OH)D3	25(OH)D
VDC	68.7±6.6	59.8±8.5	128.5±14.4
VDD	66.6±6.1	36.3±2.2	102.9±8.1

Table 3: Fetal body weights and ovarian weights following maternal vitamin D restriction

Group	Fetal Weight (FW)	Left Ovarian weight (LOW)	Right Ovarian weight (ROW)	Ave. Ovarian weight (AOW)	Ratio AOW to FW
VDC	2852.20±4.86 g	0.03±0.00 g	0.03±0.00 g	0.03±0.00 g	1.11±0.10
VDD	3044.58±183.88 g	0.03±0.00 g	0.03±0.00 g	0.03±0.00 g	1.02±0.08
<i>P-values</i>	0.34	0.53	0.47	0.47	0.50

Means with varied superscripts in a column are significantly different ($p < 0.05$)

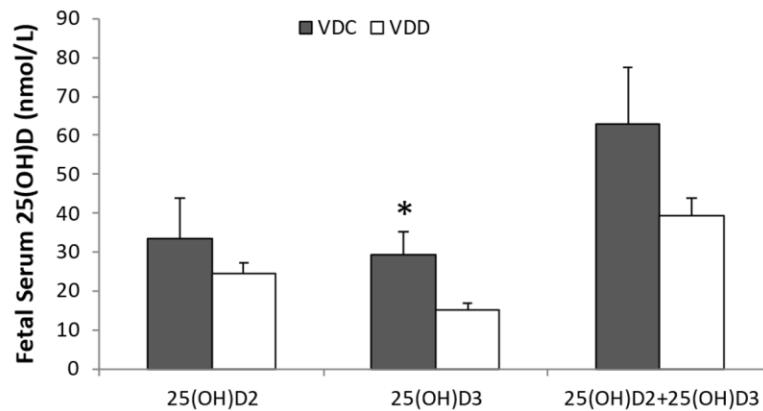


Figure 1

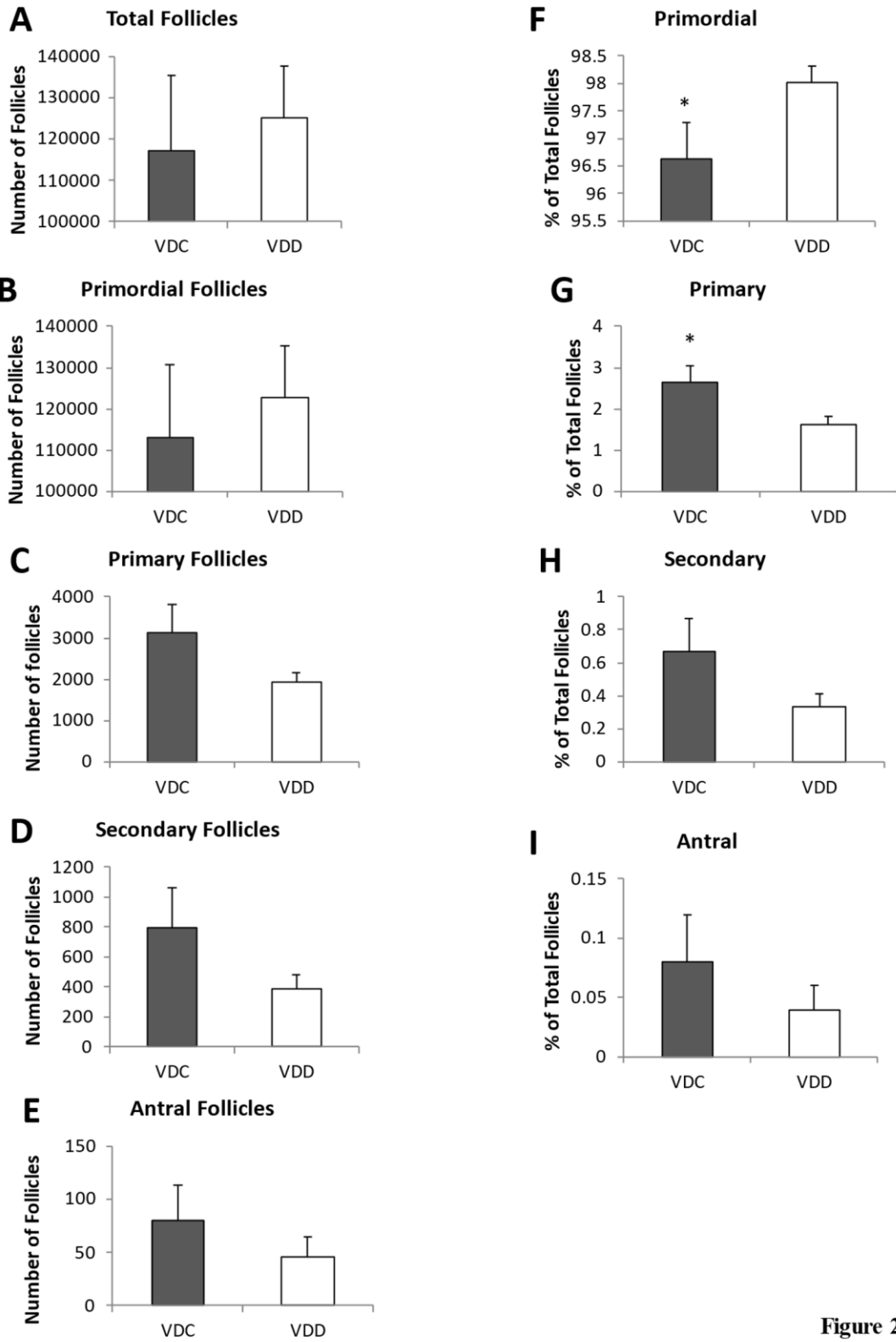


Figure 2

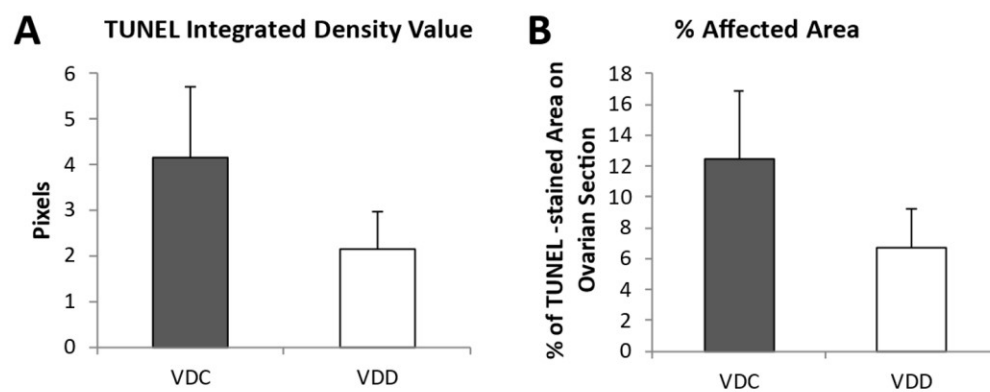
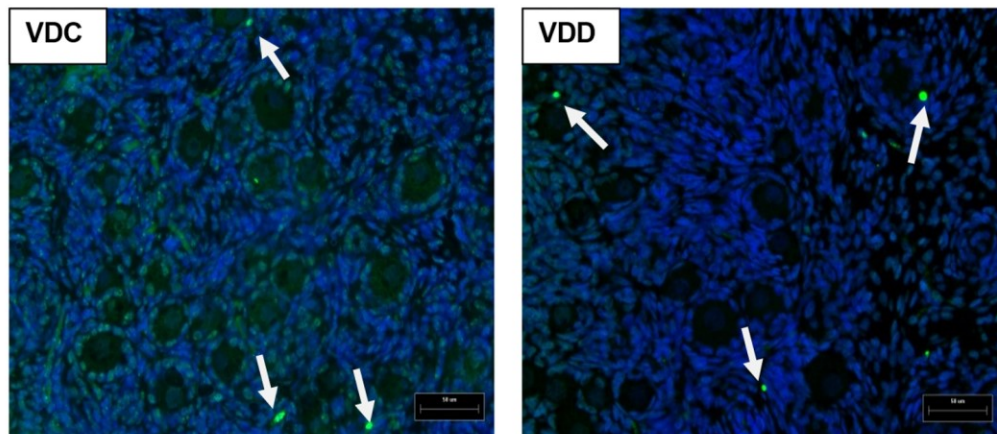


Figure 3

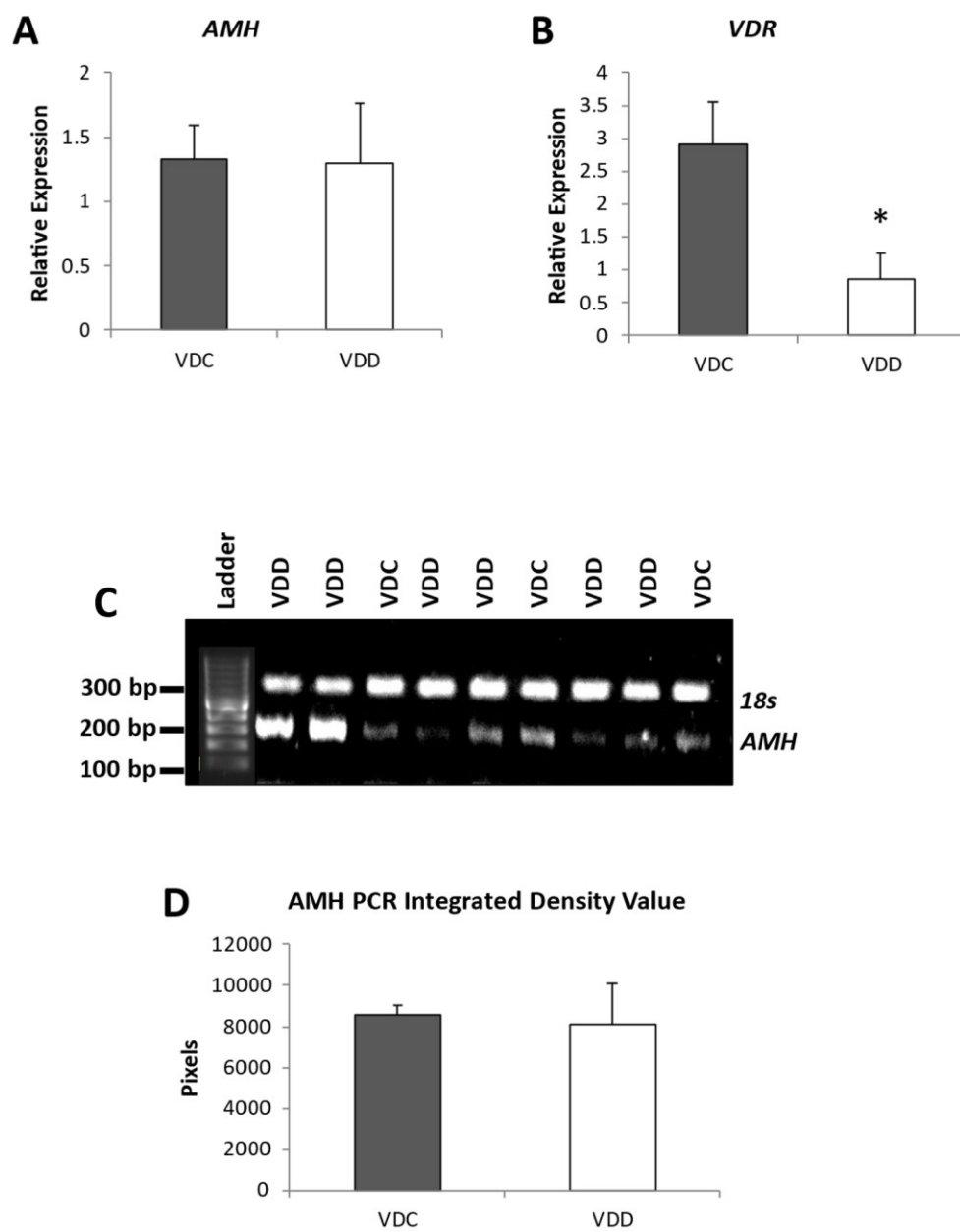
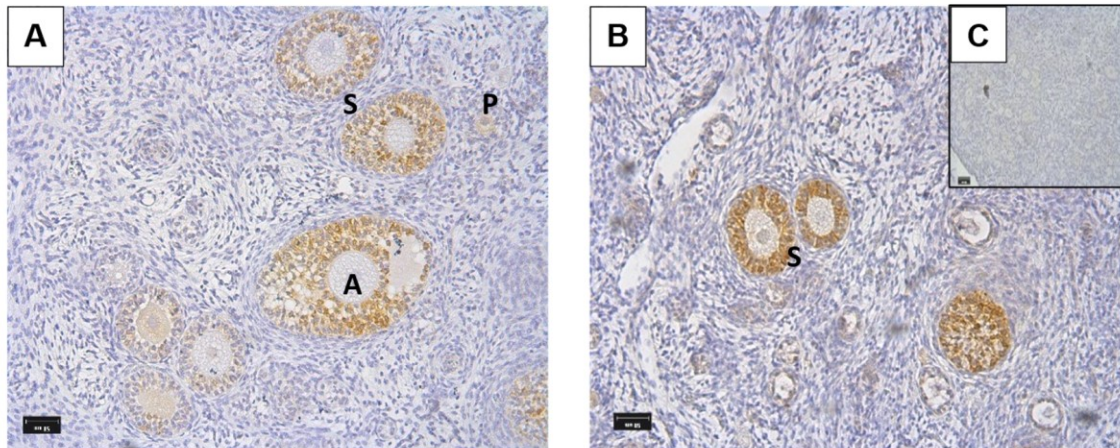
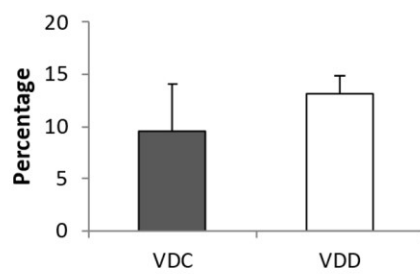


Figure 4



D % AMH DAB-stained follicles



E AMH signal/ mm2 follicles

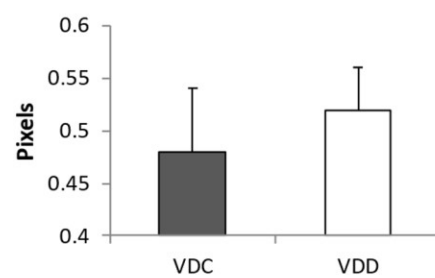


Figure 5